Examining Fluid Flow over Stretching Sheet with Variable Fluid Properties and Heat Flux

By

Iqra Arshad

A thesis
submitted in partial fulfillment of the
requirements for the degree of
Master of Science
in
Mathematics

Supervised by

Dr. Muhammad Asif Farooq

Department of Mathematics

School of Natural Sciences
National University of Sciences and Technology
H-12, Islamabad, Pakistan

2021

FORM TH-4

National University of Sciences & Technology

MS THESIS WORK

We hereby recommend that the dissertation prepared under our supervision by: IQRA ARSHAD, Regn No. 00000321453 Titled: Examining Fluid Flow over Unsteady Stretching Sheet with Variable Fluid Properties and Heat Flux be accepted in partial fulfillment of the requirements for the award of **MS** degree.

Examination Committee Members

1. Name: DR. MERAJ MUSTAFA HASHMI Signature: _____

2. Name: DR. MUJEEB UR REHMAN Signature: _____

External Examiner: DR. SHAFQAT HUSSAIN Signature: _____

Supervisor's Name DR. M. ASIF FAROOQ Signature: _____

_____ 07/10/2021

Head of Department Date

COUNTERSINGED

Date: 07.10.2021

Dean/Principal

Dedicated

to my beloved

Parents

Acknowledgement

First and foremost, I want to thank Allah for everything. Then, I would like to express gratitude to my supervisor Dr. Muhammad Asif Farooq. By helping me in overcoming through obstacles, he made it possible to complete this research within a year. I am pleased to state that working with my supervisor was an excellent opportunity for me. Lastly, I would also want to acknowledge all the unwavering trust and support that my parents, siblings and friends provided me with.

Abstract

This thesis discusses the topic of laminar flow in the boundary layer and heat transfer for MHD fluid flow owing to a stretched sheet and changing heat flux. Thermal conductivity and viscosity varies with temperature. The equations stated in PDEs govern the problem. Similarity variables are used to convert PDEs into the system of ODEs. The ODEs are then solved utilizing *bvp4c* in the MATLAB. The effects of several factors, including magnetic parameter M, Eckert number Ec, S is the unsteadiness parameter, Darcy number γ, with some other parameters that affect the temperature and velocity profiles, and the heat transfer coefficients (local Nusselt number and skin friction coefficient), are investigated. Using *bvp4c* technique, the numerical results are achieved in tabular form. Then later compared with existing research in the literature. It can be found that depending on the parameter, the local Nusselt number, momentum and thermal boundary layer thickness and skin friction coefficient all have varying effects.

Contents

List of Figures

List of Tables

Chapter 1

Introduction

1.1 Historical Background

CFD (computational fluid dynamics) has a long history that goes back to the early 1900s [1]. Richardson [2], von Neumann [3], Godunov [4] were among the first to deal with the basic problems of CFD. For an academic discussion of CFD historical perspective, see Roache [5] and Tannehill, Anderson, and Pletcher [6]. Millions of modern technological systems, such as airplanes in flight, ships at sea, cars on the road, mechanical biomedical equipment, and so on, are partly or completely based on fluid dynamics knowledge. It is important to remember that each of these machines is a miracle of engineering fluid dynamics, in which many different fundamental principles of nature are combined in a practical way to build a system that is safe, efficient, and effective.

We will mention few themes and case studies that highlight the historical evolution of fluid dynamics and provide an understanding of fluid dynamics' intellectual ideas. The laws of buoyancy have been formulated by Archmedes ($285 - 212$ B.C.) and have been utilized for submerged and floating bodies, resulting in the differential calculus. The equation of mass conservation in one-dimensional steady flow was developed by Leonardo da Vinci ($1452 - 1519$). The principles of motion and the viscosity of linear,

now known as Newtonian laws had been proposed by Isaac Newton ($1642 - 1727$), in 1687. The differential equations of motion and its integrated form, which is now known as the Bernoulli equation, had been established by Euler. The dimensional analysis was proposed by Lord Rayleigh ($1842 - 1919$). While the famous pipe experiment was reported in 1883 by Osborne Reynolds ($1842 - 1912$). It proved the significane of dimensionless Reynolds number.

1.1.1 Fluid

There are three fundamental phases in which a substance can exist that are gas, liquid, and solid. A fluid is anything that is in liquid or gas state. To distinguish between a fluid or solid, the potentiality to oppose an applied shear stress of a substance which changes its shape is utilized. A solid can deform in response to applied shear stress, however a fluid deforms continually, regardless of how small the shear force is. Stress is proportional to strain in solids, while it is proportional to strain rate in fluids. When a constant shear force is applied at a certain strain angle, a solid eventually stops deforming, but a fluid never and it reaches a certain strain rate.

1.1.2 Classification of Fluid Flows

Fluid flow problems come in a wide variety of shapes and sizes, and it iss usually easier to group them together based on some common qualities. We have listed some of the most common ones here.

1.1.3 Newtonian Fluid

Regardless of the shear forces applied to the fluid layers, the viscosity of these fluids remains constant. At constant temperature, the viscosity doesnot change. Examples are water, milk, alcohol and so on. Newtonian fluids have a shear stress plot vs.

shear rate plot at a certain temperature which is a constant slope with a straight line, independent of the shear rate. Newton's law is represented by the equation,

$$\tau = \mu \frac{\mathrm{d}u}{\mathrm{d}y} \, ,$$

and Newtonian fluids are those that foll ow it[7].

1.1.4 Non-Newtonian Fluid

Newton's law of viscosity is not followed here. Some examples of Non-Newtonian Fluid are ketchup, salt solutions, and molten polymers[7].

1.1.5 Compressible Flow

A flow is said to be compressible when density changes become significant.
Compressible flow is concerned with fluids whose density changes significantlyÂăin response to a change in pressure. Gases like air, oxygen, and nitrogen are commonly thought of as compressible fluids since their density changes significantly with changes in pressure and temperature [8].

1.1.6 Incompressible Flow

A flow is said to be incompressible if the density remains nearly constant throughout. Incompressed flow is defined as a flow in which every small volume of fluid that moves within it remains constant in density. In general, an incompressible fluid is one that has a constant density [8].

1.1.7 Steady Flow

The term steady denotes that there is no change in variable over time [9].

$$\frac{\partial}{\partial t} = 0 \quad .$$

1.1.8 Unsteady Flow

Unsteady is the exact opposite of steady. In fluid mechanics, the term "unsteady" refers to any flow that is not steady [9].

$$\frac{\partial}{\partial t} \neq 0 \quad .$$

1.1.9 One-, Two-, and Three-Dimensional Flows

One, two or three dimensional flow is considered to be based on the fact that flow varies in one, two or three fundamental dimensions [9].

1.1.10 MHD Flow

Electric fields are induced in a conducting fluid when it moves in a magnetic field, and electric currents flow. These currents are subjected to magnetic field forces, which can significantly modify the flow. In turn, the magnetic field is modified by these currents. We interact with the magnetic and fluid-dynamic phenomena in a complex way, and flow should be examined by comparing field and fluid dynamic equations. And a wide range of physical objects, from fluid metals to cosmic plasmas, cover magnetohydrodynamic applications [10].

Combining Maxwell's equation and motion equations yields a set of equations that defines MHD flow.

$$\rho \frac{\mathrm{D}\vec{V}}{\mathrm{D}t} = \vec{\nabla}.\tau + \left(\vec{J} \times \vec{B}\right) \ , \tag{1}$$

where $\vec{J}$ is representing current density.

Total magnetic field is

$$B = B + B_i \ ,$$

where B_i represents induced magnetic field.

From Ohm's Law

$$\vec{J} = \sigma \left(\vec{E} + \vec{V} \times \vec{B} \right) ,$$

where E is electrical field and σ is electrical conductivity.

Taking

$$\vec{J} \times \vec{B} = -\sigma B_0^2 u\hat{i} . \tag{2}$$

Putting (2) into (1)

$$\rho \frac{\mathrm{D}\vec{V}}{\mathrm{D}t} = \vec{\nabla}.\tau - \sigma B_0^2 u\hat{i} .$$

1.2 Boundary Layer

In 1904, Prandtl showed that it is possible to study viscous flows by dividing them into two regions: a region that has a thin layer of flow near a solid wall, which is called a boundary layer that does not neglect viscous forces and an outer region that can ignore friction [11].

1.2.1 Momentum Boundary Layer

To adhere to the no slip condition, fluid particles exbihit a zero velocity when they come into contact with a solid surface. These fluid particles affect the adjacent fluid layer particles and thus affect the next layer of fluid particles. This velocity slowing takes place at a significant distance from the flat surface where the retardation is negligible. Fluid velocity in the boundary layer vary from 0 to $0.99U_\infty$, where U_∞ is the free stream velocity.

1.2.2 Thermal Boundary Layer

A temperature field is created whenever a fluid flows past a heated surface, and the thermal boundary layer is the zone where the thermal field exists. The temperature of the layer adjacent to the surface will be the same as that of the surface, and as we travel away from the surface, the temperature will drop until it approaches the temperature of the free stream.

1.3 Conservation Laws

1.3.1 The Fluid as a Continuum

The deformable continuum includes fluids. When a material system comprises a continuous material and each particle is a continuum of matter, the system is said to be a continuum. The continuum hypothesis states that because matter is made up of molecules, a small volume can contain a vast number of molecules. Instead of the properties of each molecule at a given stage in the continuum study, we are interested in the average of these properties in a large number of molecules near each point (molecule) (fluids, in particular). The following postulate actually synthesises the concept of continuity, that is, the matter is continuously distributed in the whole imagined region, even in smallest volumes, with a large number of molecules [12].

1.3.2 Mass Conservation Law

According to this law, mass cannot be created or destroyed.[13].

$$\frac{\partial \rho}{\partial t} + \vec{\nabla}.\left(\rho \vec{V}\right) = 0\,.$$

Above is the continuity equation. It expresses mass conservation in differential form. For flows which are incompressible one can have:

$$\nabla.\vec{V} = 0\,.$$

1.3.3 Momentum Conservation Law

The cornerstone for momentum conservation is Newton's second law, $\sum F = ma$, which regulates fluid momentum. The rate of change in momentum of a body is equal to the force applied to it, according to the rule, and it happens in the same direction as the force.

$$\rho \frac{\mathrm{d}\vec{V}}{\mathrm{d}t} = \vec{\nabla}.\tau + \rho g \,,$$

where τ and g denotes the stress tensor and the body force respectively, $\frac{\mathrm{d}}{\mathrm{d}t}$ is the material time derivative.

1.3.4 Energy Conservation Law

Energy can be changed from one form to another, but the total energy in a closed system remains constant.

$$\rho C_p \frac{\mathrm{D}T}{\mathrm{D}t} = \vec{\nabla}.\left(k\vec{\nabla}T\right) + \phi \,,$$

where

$$\frac{\mathrm{D}}{\mathrm{D}t} = \frac{\partial}{\partial t} + \left(\vec{V}.\vec{\nabla}\right) \,,$$

k is the thermal conductivity, T is temperature, ϕ is the viscous dissipation function.

1.4 Non Dimensional Parameters

1.4.1 Reynolds Number (Re)

The Reynolds number refers to the ratio between inertial and viscous forces.

$$Re = \frac{uL}{\nu} = \frac{\rho u L}{\mu} \,,$$

where ρ, u and L represent the density, flow velocity and characteristic length respectively. The dynamic and kinematic viscosity are given by μ and ν.

1.4.2 Prandtl Number (Pr)

The Prandtl number is the ratio of momentum diffusivity to thermal diffusivity,

$$Pr = \frac{\nu}{\alpha} = \frac{c_p \mu}{k} ,$$

It is a dimensionless number where as k and C_p are the thermal conductivity and the specific heat respectively.

1.4.3 Nusselt Number (Nu)

The Nusselt number is defined as the ratio of convective to conductive heat transfer across a boundary.

$$Nu = \frac{\text{convective heat transfer}}{\text{conductive heat transfer}} = \frac{hL}{k} ,$$

where h is the flow's convective heat transfer coefficient, L is the characteristic length, and k is the fluid's thermal conductivity.

1.4.4 Eckert Number (Ec)

The Eckert number (Ec) is a dimensionless number. It expresses the link between a flow's kinetic energy and the boundary layer enthalpy difference to characterise heat transfer dissipation.

$$Ec = \frac{\text{Advective Transport}}{\text{Heat Dissipation}} = \frac{u^2}{C_p \Delta T} ,$$

The difference in temperature between the wall and the local temperature is given by ΔT, where as u and k are flow velocity and specific heat respectively.

1.4.5 Magnetic Parameter (M)

The ratio of Lorentz force to inertial force is the magnetic interaction parameter ,

$$M = \frac{\sigma B_0^2}{\rho a} ,$$

where B_0 is the magnetic field strength, σ is the electrical conductivity, ρ is the density.

1.4.6 Thermal Conductivity Parameter (ϵ)

The ability of a material to conduct heat is measured by its thermal conductivity. The term k is widely used to describe it. Thermal conductivity is defined by the equation

$$q = -k\vec{\nabla}T ,$$

where q is heat flux, k is the thermal conductivity and $\vec{\nabla}T$ is the temperature gradient.

1.4.7 Darcy Number (γ)

The relative effect of the medium's permeability versus its cross-sectional area is represented by the Darcy number (Da):

$$Da = \frac{K}{d^2} ,$$

where K is the permeability of the medium, d is the characteristic length.

1.4.8 Skin Friction Coefficient

It is the ratio of wall shear stress to the free stream momentum.

$$C_f = \frac{\tau_w}{\frac{1}{2}\rho v^2} ,$$

where C_f is a skin friction coefficient, ρ is the density of the fluid, v is the free stream speed. The skin shear stress on the surface is given by τ_w where as the free stream's dynamic pressure is represented by $\frac{1}{2}\rho v^2$.

1.4.9 Darcy's Law

Darcy's law is a simple proportionality relationship between the instantaneous flux through a porous medium, the medium's permeability k, the fluid's dynamic viscosity μ, and the pressure drop ∇p over a given distance, in the absence of gravitational forces and in a homogeneously permeable medium.

$$q = -\frac{k}{\mu}\nabla P \, .$$

1.4.10 Powell-Eyring Fluid Model

The Navier-Stokes equations, which are well-known governing equations, are unable to sufficiently determine the behaviour of non-Newtonian fluids. To characterise the non-Newtonian behaviour, the Powell-Eyring fluid model is used. The Powell-Eyring model is a rheological fluid with a number of benefits, including simplicity and computational ease. It is significant because it is derived from the kinetic theory of liquids.
The stress tensor for Powell-Eyring Fluid model is:

$$S = \mu A_1 + \frac{1}{\beta} sinh^{-1}\left(\frac{1}{d}A_1\right) \, ,$$

where S is the Cauchy tensor, μ is the viscosity, β and d are the material constants.

1.4.11 *bvp4c*

The *bvp4c* solver in MATLAB allows you to solve fairly complex problems in a simple and easy way. For solving nonlinear systems of equations, the algorithm uses an iteration structure. It is a finite-difference code. The residual of the continuous solution is used for mesh selection and error control. Because it is an iteration scheme, the algorithm's effectiveness will ultimately be determined by your ability to make an initial guess for the solution to the algorithm.

Chapter 2

Modeling of MHD Fluid Flow with Thermal Radiation, Variable Fluid Properties, and Heat Flux over an Unsteady Stretching Sheet

This chapter reviews the problems of laminar flow and heat transfer of MHD fluid boundary layer caused by an unstable stretching sheet with variable heat flux. Temperature is assumed to affect both viscosity and thermal conductivity. The similarity variables are used to convert the PDEs into a coupled nonlinear system of ODEs. *bvp4c* is used to solve a system of ODEs. Different parameters' effects on dimensionless velocity and temperature profiles are visually displayed and investigated. Furthermore, the results obtained using *bvp4c* are compared to previously published work from the existing literature and are determined to be in good agreement.

2.1 Mathematical Formulation

The usual Boussinesq approximation [14] is used to model the two dimensional laminar incompressible unsteady motion of a Newtonian fluid.

The specific heat at constant pressure (c_p), the electrical conductivity (σ), and the

density of a fluid (ρ) are all considered constants. The viscosity of the fluid μ and the thermal conductivity of the fluid κ are both investigated in relation to temperature.
A uniform transverse magnetic field [15]

$$B = B_0 \left(1 - at\right)^{\frac{-1}{2}},$$

has an influence on the fluid flow field, where B_0 is a constant.
The fluid motion is expected to be caused by a stretching sheet with velocity $U_x(x,t)$ that is highly dependent on x, t.
The continuity, momentum and energy equations are:

$$\frac{\partial u}{\partial x} + \frac{\partial v}{\partial y} = 0, \tag{2.1}$$

$$\frac{\partial u}{\partial t} + u\frac{\partial u}{\partial x} + v\frac{\partial u}{\partial y} = \frac{1}{\rho_\infty}\frac{\partial}{\partial y}\left(\mu\frac{\partial u}{\partial y}\right) - \frac{\sigma B^2}{\rho_\infty}u, \tag{2.2}$$

$$\frac{\partial T}{\partial t} + u\frac{\partial T}{\partial x} + v\frac{\partial T}{\partial y} = \frac{1}{\rho_\infty c_p}\frac{\partial}{\partial y}\left(\kappa\frac{\partial T}{\partial y}\right) + \frac{\mu}{\rho_\infty c_p}\left(\frac{\partial u}{\partial y}\right)^2 - \frac{1}{\rho_\infty c_p}\frac{\partial q_r}{\partial y}, \tag{2.3}$$

where u is the velocity component in x direction and v is the velocity component in the y direction, c_p is the specific heat at constant pressure, σ is the electrical conductivity, κ is the thermal conductivity, the radiative heat flux is q_r and ρ_∞ is the fluid density going away from the sheet, t is time and T is the temperature of the fluid.
Defining

$$\kappa_{eff} = \kappa\left(T\right) + \frac{16\sigma^* T_\infty^3}{3k^*}.$$

Boundary conditions that have been transformed are:

$$\begin{aligned} u = U_w, \quad v = 0, \quad -\kappa_{eff}\frac{\partial T}{\partial y} = q\left(x,t\right), \quad at \quad y = 0, \\ u \to 0, \quad T \to T_\infty, \quad as \quad y \to \infty, \end{aligned} \tag{2.4}$$

where T_∞ is the ambient temperature of fluid.
Variable heat flux [16] is assumed to influence the temperature field.

$$q\left(x,t\right) = -\kappa_{eff}\frac{\partial T}{\partial y} = T_0\frac{dx^r}{\left(1-at\right)^{m+\frac{1}{2}}}, \tag{2.5}$$

where, T_0 is the reference temperature, d and a are the positive constants, and m and r are the indices.

For radiation, the Rosseland approximation is used [17].

$$q_r = -\frac{4\sigma^*}{3k^*}\frac{\partial T^4}{\partial y}\,, \tag{2.6}$$

where k^* is the absorption coefficient and σ^* is the Stefan-Boltzmann constant.

Using Taylor series, T^4 is expanded about T_∞ and ignoring the terms of higher order, we get

$$T^4 \cong 4T_\infty^3 T - 3T_\infty^4\,.$$

The surface velocity, U_w, is

$$U_w = \frac{bx}{1-at}\,, \tag{2.7}$$

where b and a are the positive constants having dimension $[T^{-1}]$.

The similarity variables are specifically defined by:

$$\begin{aligned} \eta &= y\sqrt{\frac{b}{\nu_\infty\,(1-at)}}\,, \\ \psi &= \sqrt{\frac{\nu_\infty b}{(1-at)}}xf\,(\eta)\ , \\ \theta\,(\eta) &= \frac{T-T_\infty}{\frac{q(x,t)}{\kappa_\infty}\sqrt{\frac{\nu_\infty}{b}}\,(1-at)^{\frac{1}{2}}}\,, \end{aligned} \tag{2.8}$$

where ν_∞ denotes the ambient kinematic viscosity.

The velocity components are:

$$u = \frac{\partial\psi}{\partial y},\ \ v = -\frac{\partial\psi}{\partial x}\,.$$

The surface temperature T_w is:

$$T_w = T_\infty + T_0\left(\frac{dx^r}{\kappa_\infty\sqrt{\frac{b}{\nu_\infty}}}\right)(1-at)^{-m}\,\theta\,(0)\ .$$

It is assumed that variable thermal conductivity κ and the variable viscosity μ change with temperature [18].

$$\mu = \mu_\infty e^{-\alpha\theta},$$
$$\kappa = \kappa_\infty \left(1 + \epsilon\theta\right),$$

where the dimensionless viscosity parameter, thermal conductivity away from the surface, thermal conductivity parameter, and ambient viscosity are represented by α, κ_∞, ϵ, and μ_∞, respectively.

Putting Eq. (2.8) in Eqs. (2.1)-(2.4),

$$e^{-\alpha\theta}\left(-\alpha\theta^{'}f^{''} + f^{'''}\right) - \mathrm{M}f^{'} - \mathrm{S}f^{'} - \mathrm{S}\frac{1}{2}\eta f^{''} - f^{'^2} + ff^{''} = 0, \tag{2.9}$$

$$\frac{1}{\mathrm{Pr}}\left(\epsilon\theta^{'^2} + \left(1 + \epsilon\theta + \mathrm{R}\right)\theta^{''}\right) - rf^{'}\theta + f\theta^{'} - \frac{\theta^{'}}{2}\mathrm{S}\eta - m\mathrm{S}\theta + \mathrm{Ec}f^{''^2}e^{-\alpha\theta} = 0. \tag{2.10}$$

The following boundary conditions are modified and given as:

$$\begin{aligned} f\left(0\right) = 0, \quad f^{'}\left(0\right) = 1\,, \\ \theta^{'}\left(0\right) = \frac{-1}{\left(\left(1 + \epsilon\theta\left(0\right)\right) + \mathrm{R}\right)}\,, \\ f^{'} \to 0, \quad \theta \to 0, \quad as \quad \eta \to \infty\,. \end{aligned} \tag{2.11}$$

The resulting parameters are:

$$\mathrm{M} = \frac{\sigma B_0^2}{b\rho_\infty}\,, \qquad \mathrm{S} = \frac{a}{b}\,, \qquad \mathrm{R} = \frac{16\sigma^* T_\infty^3}{3\kappa_\infty k^*}\,,$$
$$\mathrm{Ec} = \frac{\kappa_\infty b^{\frac{5}{2}}}{d\sqrt{\nu_\infty}c_p T_0}\,, \quad \mathrm{Pr} = \frac{\mu_\infty c_p}{\kappa_\infty}\,,$$

2.1.1 Skin Friction Coefficient

Defining skin friction coefficient as [21]:

$$Cf_x = \frac{2\tau_w}{\rho U_w^2}\,, \tag{2.12}$$

where

$$\tau_w = \left(-\mu\left(\frac{\partial u}{\partial y}\right)\right)\Big|_{y=0} . \tag{2.13}$$

Inserting Eq. (2.7) and Eq. (2.13) in Eq. (2.12)

$$Cf_x Re_x^{\frac{1}{2}}/2 = -e^{-\alpha\theta(0)} f''(0) . \tag{2.14}$$

2.1.2 Local Nusselt Number

Defining local Nusselt number as:

$$Nu_x = \frac{xq(x,t)}{\kappa_\infty (T_w - T_\infty)} . \tag{2.15}$$

$$\text{where} \quad q(x,t) = T_0 \frac{dx^r}{(1-at)^{m+\frac{1}{2}}} ,$$

$$T_w - T_\infty = T_0 \left(\frac{dx^r}{\kappa_\infty \sqrt{\frac{b}{\nu_\infty}}}\right)(1-at)^{-m}\,\theta(0) ,$$

Inserting Eq. (2.5) in Eq. (2.15)

$$Nu_x (Re_x)^{\frac{-1}{2}} = \frac{1}{\theta(0)} . \tag{2.16}$$

where, $Re_x = \frac{U_w x}{\nu_\infty}$ represents the local Reynolds number.

2.2 Numerical Solution

In **Table 2.1**, the consequences of different parameters on Cf_x and Nu_x are investigated. It can be seen that Cf_x grows as the M is increased. For increasing values of R, we see that Nu_x increases. One can observe that Nu_x decreases with rising Ec values and Cf_x declines as α increases. It can be noted that as the value of S varies, Nu_x rises. There is a slight increase in Nu_x as ϵ varies.

M	R	Ec	α	S	ϵ	Variable Case	
						$-e^{-\alpha\theta(0)}f''(0)$	$\frac{1}{\theta(0)}$
0.4	0.2	0.2	0.2	0.2	0.2	1.1799	1.4485
0.8	0.2	0.2	0.2	0.2	0.2	1.3197	1.3941
1.2	0.2	0.2	0.2	0.2	0.2	1.4446	1.3479
0.3	**0.4**	0.2	0.2	0.2	0.2	1.1439	1.5463
0.3	**0.8**	0.2	0.2	0.2	0.2	1.1471	1.6915
0.3	**1.2**	0.2	0.2	0.2	0.2	1.1496	1.8171
0.3	0.2	**0.4**	0.2	0.2	0.2	1.1367	1.3633
0.3	0.2	**0.8**	0.2	0.2	0.2	1.1263	1.2000
0.3	0.2	**1.2**	0.2	0.2	0.2	1.1160	1.0728
0.3	0.2	0.2	**0.4**	0.2	0.2	1.0824	1.4488
0.3	0.2	0.2	**0.8**	0.2	0.2	1.9635	1.4162
0.3	0.2	0.2	**1.2**	0.2	0.2	0.8458	1.3796
0.3	0.2	0.2	0.2	**0.4**	0.2	1.2053	1.6005
0.3	0.2	0.2	0.2	**0.8**	0.2	1.3234	1.8281
0.3	0.2	0.2	0.2	**1.2**	0.2	1.4327	2.0208
0.3	0.2	0.2	0.2	0.2	**0.4**	1.1427	1.5032
0.3	0.2	0.2	0.2	0.2	**0.8**	1.1440	1.5724
0.3	0.2	0.2	0.2	0.2	**1.2**	1.1451	1.6323

Table 2.1: Variable Case

Table 2.2 shows that as M rises, Cf_x rises and Nu_x slightly decreases. When R is changed, Nu_x rises. When Ec varies, Nu_x falls. When S changes, Nu_x and Cf_x increase slightly.

M	R	Ec	S	Constant Case (α=$\epsilon = 0$)	
				$-f''(0)$	$\frac{1}{\theta(0)}$
0.4	0.2	0.2	0.2	1.1523	1.4523
0.8	0.2	0.2	0.2	1.2310	1.4246
1.2	0.2	0.2	0.2	1.3051	1.3991
0.3	**0.4**	0.2	0.2	1.1109	1.4166
0.3	**0.8**	0.2	0.2	1.1109	1.5151
0.3	**1.2**	0.2	0.2	1.1109	1.6037
0.3	0.2	**0.4**	0.2	1.1109	1.5191
0.3	0.2	**0.8**	0.2	1.1109	1.4188
0.3	0.2	**1.2**	0.2	1.1109	1.3309
0.3	0.2	0.2	**0.4**	1.0803	1.3961
0.3	0.2	0.2	**0.8**	1.1411	1.5331
0.3	0.2	0.2	**1.2**	1.2003	1.6532

Table 2.2: Constant Case ($\alpha = 0, \epsilon = 0$)

2.3 Graphical Analysis

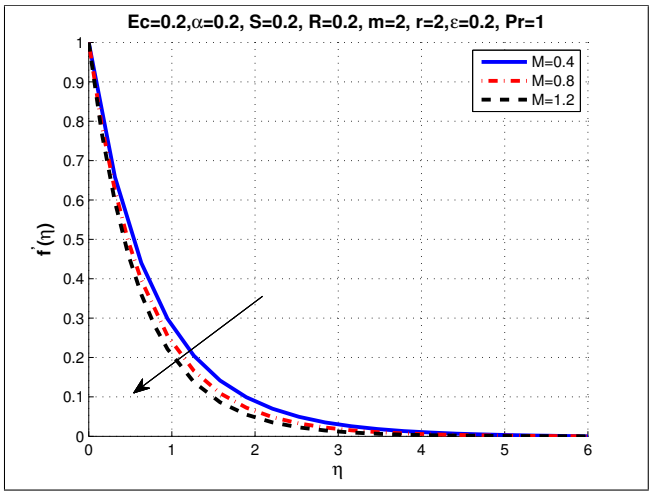

(a)

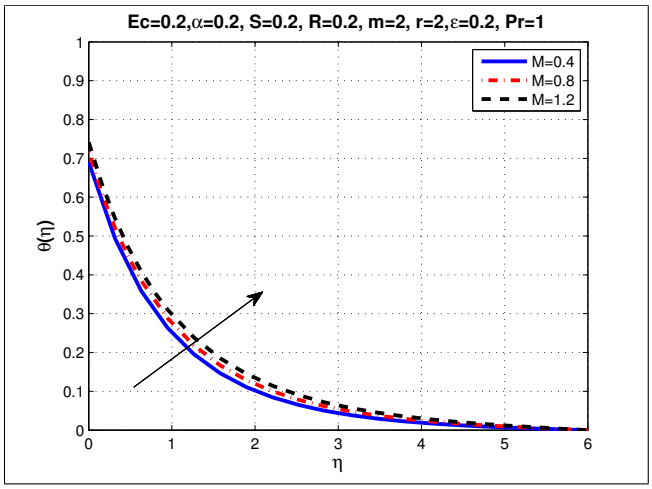

(b)

Figure 2.1: (a) Analysis of velocity for M and its distribution. (b) Analysis of temperature for M and its distribution.

From **Figure 2.1(a)** it can be seen that $f^{'}(\eta)$ and momentum boundary layer thickness both reduces with M. It can be observed from **Figure 2.1(b)** that $\theta(\eta)$ rises with a slight increase in boundary layer thickness, as the parameter M is raised.

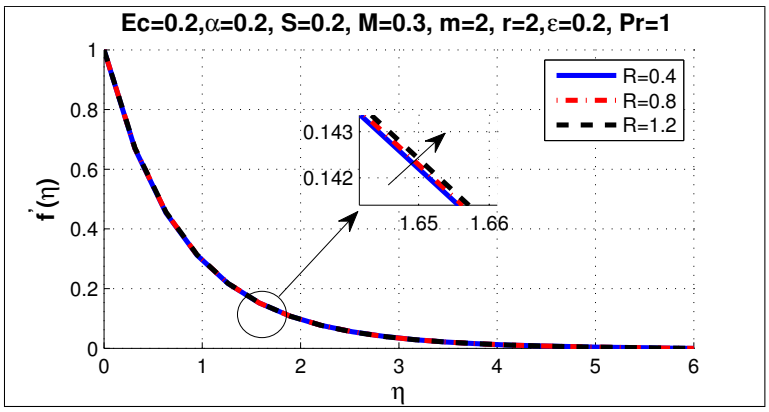

(a)

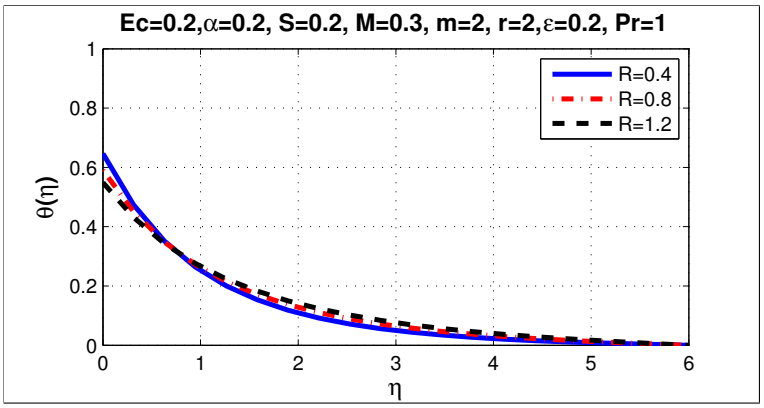

(b)

Figure 2.2: (a) Analysis of velocity for R and its distribution. (b) Analysis of temperature for R and its distribution.

The $f^{'}(\eta)$ increases as R is increased, as seen in **Figure 2.2(a)**. As R is increased, $\theta(\eta)$ decreases, as seen in **Figure 2.2(b)**.

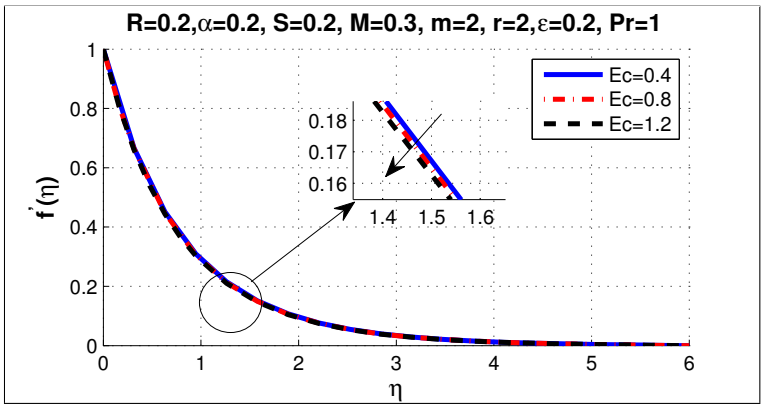

(a)

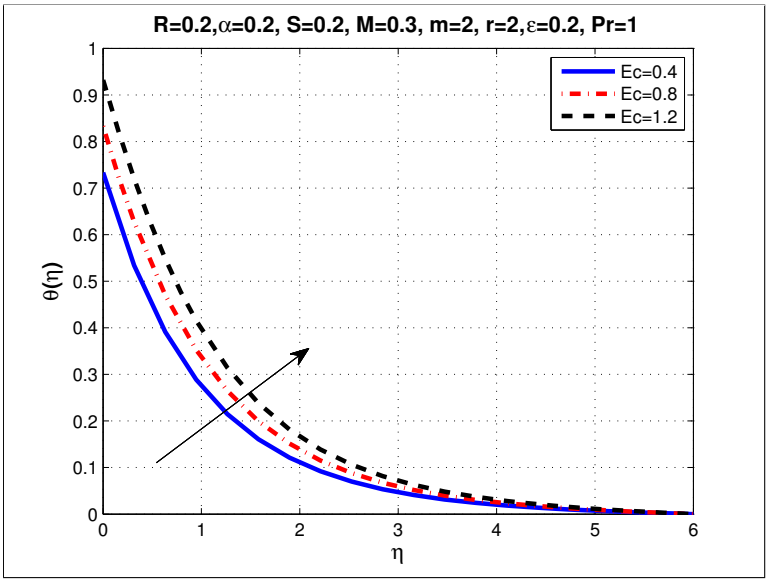

(b)

Figure 2.3: (a) Analysis of velocity for Ec and its distribution. (b) Analysis of temperature for Ec and its distribution.

Figure 2.3(a) shows how Ec affects the dimensionless velocity and dimensionless temperature. With rising values of Ec it can be shown that $f^{'}(\eta)$ decreases. The effect of Ec on $\theta(\eta)$ can be seen in **Figure 2.3(b)**. As Ec is increased, $\theta(\eta)$ and the thickness of the thermal boundary layer both increase.

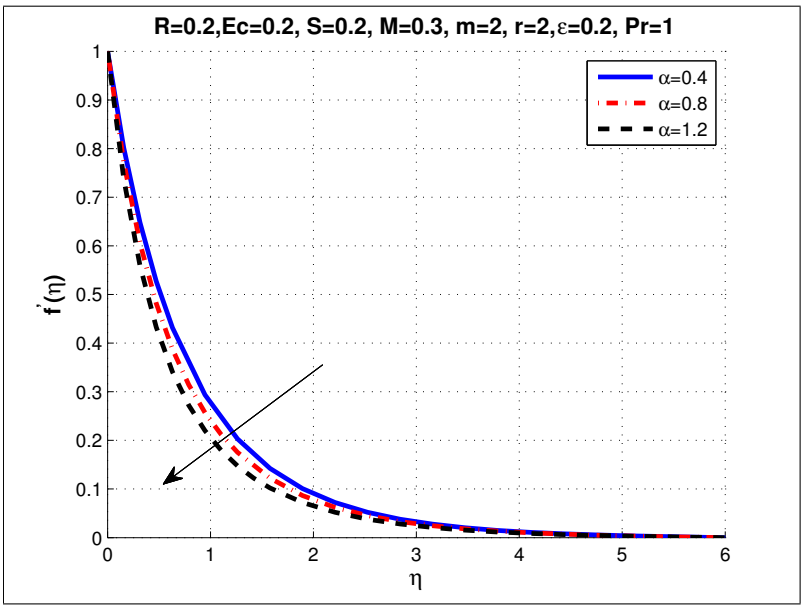

(a)

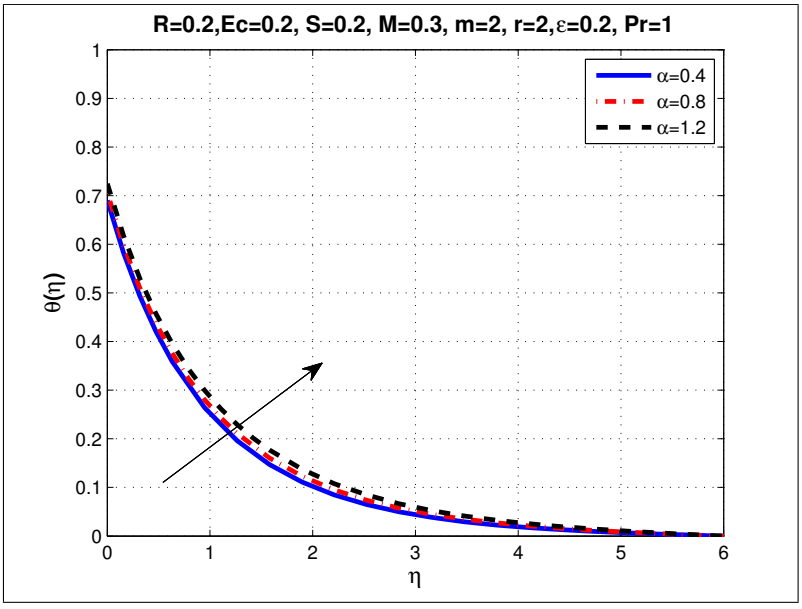

(b)

Figure 2.4: (a) Analysis of velocity for α and its distribution. (b) Analysis of temperature for α and its distribution.

Figures 2.4(a) and (b) illustrate the effects of the parameter α on $f^{'}(\eta)$ and $\theta(\eta)$. The dimensionless velocity and momentum boundary layer thicknesse decrease as α increases, while the dimensionless temperature increases.

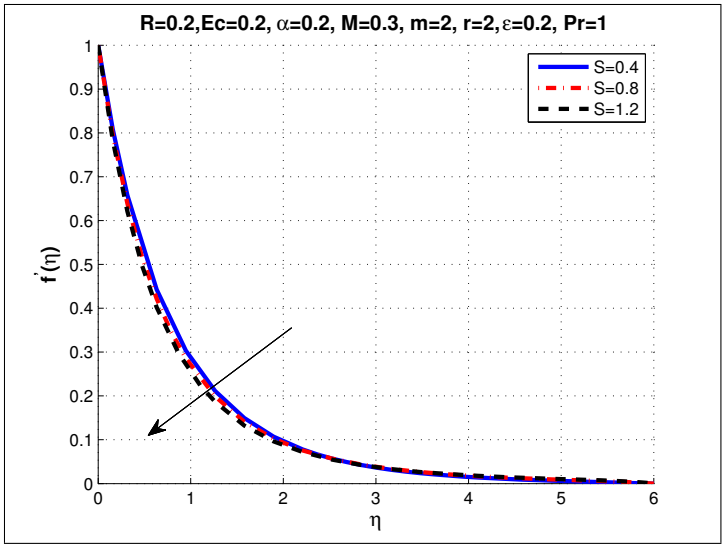

(a)

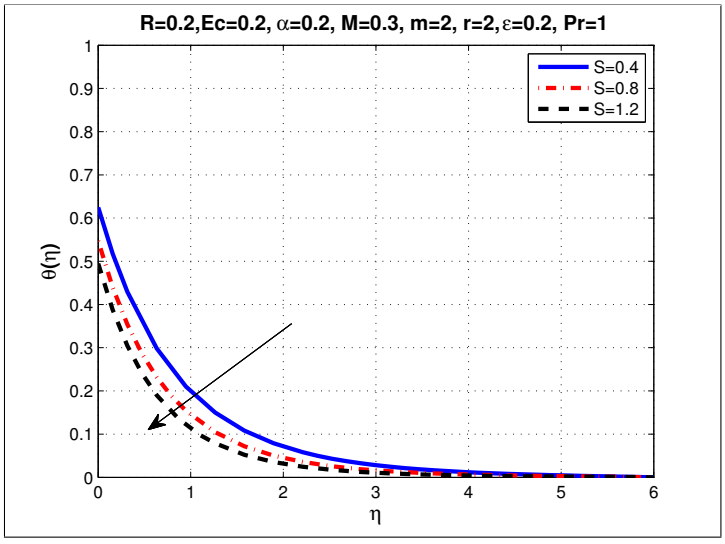

(b)

Figure 2.5: (a) Analysis of velocity for S and its distribution. (b) Analysis of temperature for S and its distribution.

Figure 2.5(a) depicts the effects of S on the velocity field. As S increases, the $f^{'}(\eta)$ decreases. In **Figure 2.5(b)**, the increasing values of S can be observed to reduce thermal boundary layer thickness and decrease dimensionless temperature.

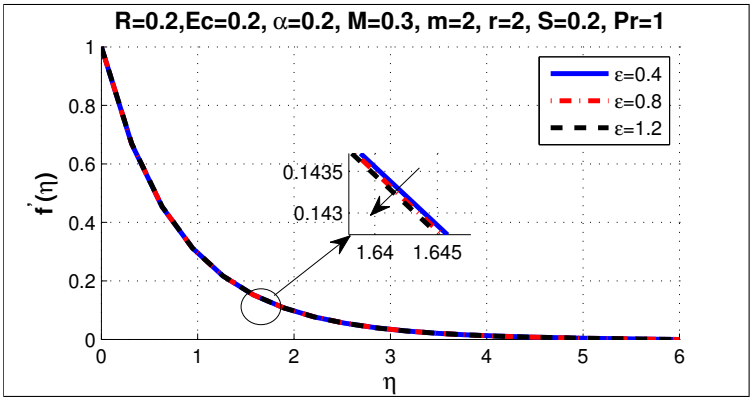

(a)

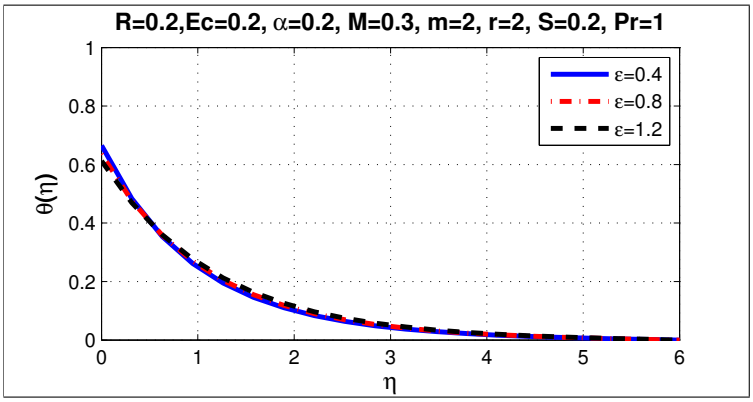

(b)

Figure 2.6: (a) Analysis of velocity for ϵ and its distribution. (b) Analysis of temperature for ϵ and its distribution.

$f^{'}(\eta)$ increases with increasing ϵ, as seen in **Figure 2.6(a)**. **Figure 2.6(b)** shows that as ϵ increases, $\theta(\eta)$ falls.

Chapter 3

Powell-Eyring MHD Fluid Flow with Variable Fluid Properties and Heat Flux over an unsteady Stretching Sheet

Now we will provide an extension to Chapter 2. And the analysis used in the Chapter 2 will be presented for the Powell-Eyring Fluid here.

3.1 Mathematical Formulation

In this case, a non Newtonian MHD flow in two dimensions is being considered. The Powell-Eyring fluid is carried on a stretched sheet with a changing heat flux.
Applying a uniform transverse magnetic field $B = B_0 (1 - at)^{\frac{-1}{2}}$ to the fluid.
The tensor components for Powell-Eyring fluid are:

$$S_{xx} = 2\mu \frac{\partial u}{\partial x} + \frac{2}{\beta d} \frac{\partial u}{\partial x} - \frac{1}{6\beta d^3} \left(2 \frac{\partial u}{\partial x} \right)^3,$$

$$S_{yx} = \mu \left(\frac{\partial v}{\partial x} + \frac{\partial u}{\partial y} \right) + \frac{1}{\beta d} \left(\frac{\partial v}{\partial x} + \frac{\partial u}{\partial y} \right) - \frac{1}{6\beta d^3} \left(\frac{\partial v}{\partial x} + \frac{\partial u}{\partial y} \right)^3.$$

The equations of continuity, momentum and energy are:

$$\frac{\partial u}{\partial x}+\frac{\partial v}{\partial y}=0, \tag{3.1}$$

$$\frac{\partial u}{\partial t}+u\frac{\partial u}{\partial x}+v\frac{\partial u}{\partial y}=\frac{1}{\rho_\infty}\frac{\partial}{\partial y}\left(\mu\frac{\partial u}{\partial y}\right)+\frac{1}{\rho_\infty\beta d}\frac{\partial^2 u}{\partial y^2} - \frac{1}{2\rho_\infty\beta d^3}\left(\frac{\partial u}{\partial y}\right)^2\left(\frac{\partial^2 u}{\partial y^2}\right)-\frac{\mu u}{\rho_\infty K}-\frac{\sigma B^2}{\rho_\infty}u, \tag{3.2}$$

$$\frac{\partial T}{\partial t}+u\frac{\partial T}{\partial x}+v\frac{\partial T}{\partial y}=\frac{1}{\rho_\infty C_p}\frac{\partial}{\partial y}\left(\kappa\frac{\partial T}{\partial y}\right)+\frac{\mu}{\rho_\infty C_p}\left(\frac{\partial u}{\partial y}\right)^2-\frac{1}{\rho_\infty C_p}\frac{\partial q_r}{\partial y}. \tag{3.3}$$

Defining

$$\kappa_{eff}=\kappa\left(T\right)+\frac{16\sigma^* T_\infty^3}{3k^*}.$$

The boundary conditions corresponding to considered model are,

$$\begin{aligned} &u=U_w, \qquad v=0, \qquad -\kappa_{eff}\frac{\partial T}{\partial y}=q\left(x,t\right), \qquad \text{at} \quad y=0,\\ &u\to 0, \qquad T\to T_\infty, \quad as \quad y\to\infty. \end{aligned} \tag{3.4}$$

where T_∞ represents ambient fluid temperature.

For variable heat flux, Liu and Megahed [16] suggested the following formula:

$$q\left(x,t\right)=-\kappa_{eff}\frac{\partial T}{\partial y}=T_0\frac{dx^r}{\left(1-at\right)^{m+\frac{1}{2}}}\,. \tag{3.5}$$

The surface velocity is U_w and can be defined as:

$$U_w=\frac{bx}{1-at}\,, \tag{3.6}$$

where to maintain the dimensionality of the U_w velocity provided above, both the positive constants a and b have dimension $[T^{-1}]$.

The velocity components are, $u=\frac{\partial\psi}{\partial y}$ and $v=-\frac{\partial\psi}{\partial x}$.

The similarity variables are defined as:

$$\begin{aligned}\eta &= y\sqrt{\frac{b}{\nu_\infty\left(1-at\right)}}\,,\\ \psi &= \sqrt{\frac{\nu_\infty b}{\left(1-at\right)}}xf\left(\eta\right),\\ \theta\left(\eta\right) &= \frac{T-T_\infty}{\frac{q(x,t)}{K_\infty}\sqrt{\frac{\nu_\infty}{b}}\left(1-at\right)^{\frac{1}{2}}}\,,\end{aligned} \tag{3.7}$$

where ν_∞ is the ambient kinematic viscosity .

3.1.1 Case A: Variable Fluid Properties

Assume that the variable μ and variable thermal conductivity κ change with temperature as well,

$$\mu = \mu_\infty e^{-\alpha\theta}\,,$$

$$\kappa = \kappa_{\infty(1+\epsilon\theta)}\,.$$

Inserting Eq. (3.7) into Eqs. (3.1)-(3.4), we get

$$\begin{aligned}e^{-\alpha\theta}\left(-\alpha\theta f^{''}+f^{'''}\right)+\mathrm{N}f^{'''}-\mathrm{N}\lambda f^{''2}f^{'''}-\gamma e^{-\alpha\theta}f^{'}\\ -\mathrm{M}f^{'}-\mathrm{S}f^{'}-\frac{1}{2}\mathrm{S}\eta f^{''}-f^{'2}+ff^{''}=0,\end{aligned} \tag{3.8}$$

$$\frac{1}{\mathrm{Pr}}\left(\epsilon\theta^{'2}+\left(1+\epsilon\theta+\mathrm{R}\right)\theta^{''}\right)-rf^{'}\theta+f\theta^{'}-\frac{\theta^{'}}{2}\mathrm{S}\eta-\mathrm{Sm}\theta+\mathrm{Ec}e^{-\alpha\theta}f^{''2}=0. \tag{3.9}$$

Boundary conditions that have been transformed are:

$$\begin{aligned}&f\left(0\right)=0\,,\quad f^{'}\left(0\right)=1\,,\quad \theta^{'}\left(0\right)=\frac{-1}{1+\epsilon\theta\left(0\right)+\mathrm{R}}\,,\\ &f^{'}\to 0\,,\quad \theta\to 0\,,\qquad \eta\longrightarrow\infty.\end{aligned} \tag{3.10}$$

The parameters we get are:

$$N = \frac{1}{\mu_\infty \beta d}\,, \qquad \lambda = \frac{b^3 x^2}{2d^2 \nu_\infty \left(1-at\right)^3}\,,$$
$$S = \frac{a}{b}\,, \qquad \gamma = \frac{\mu_\infty}{\rho_\infty K b}\left(1-at\right)\,,$$
$$M = \frac{\sigma B_0^2}{b\rho_\infty}\,, \qquad Pr = \frac{\mu_\infty C_p}{K_\infty}\,,$$
$$Ec = \frac{K_\infty b^{\frac{5}{2}}}{d\sqrt{\nu_\infty} C_p T_0}, \qquad R = \frac{16\sigma^* T_\infty^3}{3K_\infty k^*}\,.$$

The physical quantities of the interest are:

Skin Friction Coefficient

Defining skin friction coefficient C_{fx} [21] as:

$$Cf_x = \frac{2\tau_w}{\rho U_w^2}\,, \tag{3.11}$$

where

$$\tau_w = \left(\mu\frac{\partial u}{\partial y} + \frac{1}{\beta d}\frac{\partial u}{\partial y} - \frac{1}{6\beta d^3}\left(\frac{\partial u}{\partial y}\right)^3\right)\,. \tag{3.12}$$

Inserting Eq.(3.6) and Eq.(3.12) into Eq.(3.11) yields the following expression

$$\frac{Cf_x Re_x^{\frac{1}{2}}}{2} = f''\left(0\right)\left\{e^{-\alpha\theta(0)} + N - \frac{N\lambda}{3}f'^2\left(0\right)\right\}\,. \tag{3.13}$$

Local Nusselt Number

Defining local Nusselt number Nu_x as:

$$Nu_x = \frac{xq\left(x,t\right)}{\kappa_\infty\left(T_w - T_\infty\right)}\,, \tag{3.14}$$

$$\text{where} \quad q\left(x,t\right) = T_0\frac{dx^r}{\left(1-at\right)^{m+\frac{1}{2}}}\,,$$
$$T_w - T_\infty = T_0\left(\frac{dx^r}{\kappa_\infty\sqrt{\frac{b}{\nu_\infty}}}\right)\left(1-at\right)^{-m}\theta\left(0\right)\,,$$

Inserting Eq.(3.5) into Eq.(3.14) gives:

$$Nu_x \left(Re_x\right)^{\frac{-1}{2}} = \frac{1}{\theta\left(0\right)} \,. \tag{3.15}$$

where the local Reynolds number is defined as $Re_x = \frac{U_w x}{\nu}$.

3.1.2 Case B: Constant Fluid Properties

For the constant case, take $\alpha = 0$ and $\epsilon = 0$,

and set

$$B = B_0, \quad \mu = \mu_\infty, \quad K = K_\infty \,.$$

Inserting Eq.(3.7) into Eqs.(3.1)-(3.4), we get

$$f''' - \mathrm{M}f' - \mathrm{S}f' - \mathrm{S}\frac{1}{2}\eta f'' - f'^2 + ff'' = 0, \tag{3.16}$$

$$\frac{1}{\mathrm{Pr}}\left(\left(1+\mathrm{R}\right)\theta''\right) + \mathrm{Ec}f''^2 - \frac{\theta'}{2}\mathrm{S}\eta - \mathrm{S}\theta m - rf'\theta + f\theta' = 0. \tag{3.17}$$

Boundary condition that have been transformed are:

$$\begin{aligned} f\left(0\right) = 0 \,, \quad f'\left(0\right) = 1 \,, \quad \theta'\left(0\right) = -\frac{1}{1+R} \,, \\ f' \to 0 \,, \quad \theta \to 0 \,, \quad as \quad \eta \to \infty \,. \end{aligned} \tag{3.18}$$

The parameters we get are:

$$\begin{aligned} S = \frac{a}{b} \,, \qquad & M = \frac{\sigma B_0^2}{b\rho_\infty}\left(1-at\right) \,, \quad Pr = \frac{\mu_\infty C_p}{K_\infty} \,, \\ Ec = \frac{K_\infty b^{\frac{5}{2}}}{d\sqrt{\nu_\infty} C_p T_0} \,, \quad & R = \frac{16\sigma^* T_\infty^3}{3K_\infty k^*} \,. \end{aligned}$$

The physical quantities of the interest are:

Skin Friction Coefficient

Defining skin friction coefficient C_{fx} [21] as:

$$C_{f_x} = \frac{2\tau_w}{\rho U_w^2}, \tag{3.19}$$

where

$$\tau_w = \left(\mu \frac{\partial u}{\partial y} + \frac{1}{\beta d} \frac{\partial u}{\partial y} - \frac{1}{6\beta d^3} \left(\frac{\partial u}{\partial y} \right)^3 \right), \tag{3.20}$$

Inserting Eq.(3.6) and Eq.(3.20) into Eq.(3.19) yields the following expression

$$C f_x Re_x^{\frac{1}{2}} = f^{''}(0) \left\{ 1 + N - \frac{N\lambda}{3} f^{''2}(0) \right\}. \tag{3.21}$$

The local Nusselt number

Defining local Nusselt number Nu_x as:

$$Nu_x = \frac{xq}{\kappa_\infty (T_w - T_\infty)}, \tag{3.22}$$

where

$$q(x,t) = T_0 \frac{dx^r}{(1-at)^{m+\frac{1}{2}}},$$

$$T_w - T_\infty = T_0 \left(\frac{dx^r}{\kappa_\infty \sqrt{\frac{b}{\nu_\infty}}} \right) (1-at)^{-m} \theta(0),$$

Inserting Eq. (3.5) into Eq.(3.22) yields the following expressions

$$Nu_x (Re_x)^{\frac{-1}{2}} = \frac{1}{\theta(0)}. \tag{3.23}$$

where the local Reynolds number is defined as $Re_x = \frac{U_w x}{\nu}$.

3.2 Numerical Process

3.2.1 Comparison of Skin Friction

M	Prasad et al.[19]	Megahed et al.[20]	Present Work
0.0	1.0000	1.0000	1.0000
0.5	1.22490	1.2289	1.2247
1.0	1.41440	1.4143	1.4142
1.5	1.58100	1.5810	1.5811
2.0	1.73200	1.7319	1.7321

Table 3.1: For $\alpha = S = 0$, Comparing the skin friction coefficient $f''(0)$

A comparison of skin friction coefficient between earlier results presented by Prasad et al [19], Megahed et al [20] and present work is done in which for the variation of M at 1.5 and 2 the highest value is obtained for our work. Moreover, at 1 the maximum value is found in Prasad results whereas Megahed results show maximum value of skin friction coefficient at 0.5. The bar graph for the result is displayed in **Figure 3.1**.

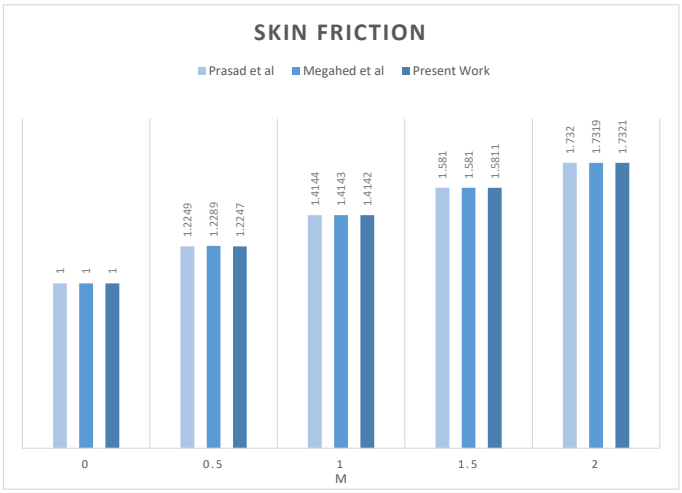

Figure 3.1: Bar graph when $\alpha = S = 0$, for the comparison of skin friction coefficient

3.2.2 Cases for Fluid Properties

Now the transformed ODEs will be converted into a system of first-order. Then, using bvp4c, a numerical analysis of the aur system will be obtained.

3.2.3 Case A: Variable Fluid Properties

From Eq.(3.8) & (3.9) the system of first order is:

$$
\begin{aligned}
y_1 = f \qquad & \Rightarrow y_1^{'} = f^{'} = y_2 \ , \\
y_2 = f^{'} \qquad & \Rightarrow y_2^{'} = f^{''} = y_3 \ , \\
y_3 = f^{''} \qquad & \Rightarrow y_3^{'} = f^{'''} = \frac{1}{1 + e^{\alpha y_4}\mathrm{N} - \mathrm{N}\lambda y_3^2 e^{\alpha y_4}} \\
& \quad \{\alpha y_5 y_3 + \gamma y_2 + e^{\alpha y_4} \\
& \quad \left(\mathrm{M}y_2 + y_2^2 + \mathrm{S}y_2 + \frac{1}{2}\mathrm{S}\eta y_3 - y_1 y_3\right)\Big\} \ , \\
y_4 = \theta \qquad & \Rightarrow y_4^{'} = \theta^{'} = y_5 \ , \\
y_5 = \theta^{'} \qquad & \Rightarrow y_5^{'} = \theta^{''} = \frac{1}{(1 + \epsilon y_4 + \mathrm{R})}\left(-\epsilon y_5^2 + r\mathrm{Pr}y_2 y_4\right. \\
& \quad \left. -\mathrm{Pr}y_1 y_5 + Pry_5\frac{\mathrm{S}}{2}\eta + m\mathrm{PrS}y_4 - \mathrm{PrEc}e^{-\alpha y_4} y_3^2\right) \ .
\end{aligned}
\tag{3.24}
$$

Table 3.2 shows that, both Nu_x and C_{fx} show a slight decrease in the behaviour with the increasing λ. When N increases, C_{fx} slightly increases. As γ varies, their is a slight growth in C_{fx} but a slight reduction of the Nu_x. It can be observed that C_{fx} increases for M and Nu_x increases with R. For Ec and α the Nu_x shows a decline in behaviour. In the case of S, Nu_x rises, whereas C_{fx} rises slightly. And, Nu_x increases as ϵ is increased.

λ	N	γ	M	R	Ec	α	S	ϵ	r	m	Pr	Variable Case (bvp4c)	
												$Cf_x\sqrt{Re_x}$	$\frac{Nu_x}{\sqrt{Re_x}}$
0.4	0.1	0.2	0.3	0.2	0.2	0.2	0.2	0.2	2	2	1	1.2693	1.4553
0.8	0.1	0.2	0.3	0.2	0.2	0.2	0.2	0.2	2	2	1	1.2603	1.4512
1.2	0.1	0.2	0.3	0.2	0.2	0.2	0.2	0.2	2	2	1	1.2509	1.4468
0.2	**0.4**	0.2	0.3	0.2	0.2	0.2	0.2	0.2	2	2	1	1.4500	1.5090
0.2	**0.8**	0.2	0.3	0.2	0.2	0.2	0.2	0.2	2	2	1	1.6587	1.5586
0.2	**1.2**	0.2	0.3	0.2	0.2	0.2	0.2	0.2	2	2	1	1.8450	1.5947
0.2	0.1	**0.4**	0.3	0.2	0.2	0.2	0.2	0.2	2	2	1	1.3401	1.4324
0.2	0.1	**0.8**	0.3	0.2	0.2	0.2	0.2	0.2	2	2	1	1.4620	1.3884
0.2	0.1	**1.2**	0.3	0.2	0.2	0.2	0.2	0.2	2	2	1	1.5718	1.3503
0.2	0.1	0.2	**0.4**	0.2	0.2	0.2	0.2	0.2	2	2	1	1.3107	1.4437
0.2	0.1	0.2	**0.8**	0.2	0.2	0.2	0.2	0.2	2	2	1	1.4491	1.3945
0.2	0.1	0.2	**1.2**	0.2	0.2	0.2	0.2	0.2	2	2	1	1.5738	1.3520
0.2	0.1	0.2	0.3	**0.4**	0.2	0.2	0.2	0.2	2	2	1	1.2756	1.5389
0.2	0.1	0.2	0.3	**0.8**	0.2	0.2	0.2	0.2	2	2	1	1.2792	1.6826
0.2	0.1	0.2	0.3	**1.2**	0.2	0.2	0.2	0.2	2	2	1	1.2819	1.8068
0.2	0.1	0.2	0.3	0.2	**0.4**	0.2	0.2	0.2	2	2	1	1.2674	1.3560
0.2	0.1	0.2	0.3	0.2	**0.8**	0.2	0.2	0.2	2	2	1	1.2555	1.1923
0.2	0.1	0.2	0.3	0.2	**1.2**	0.2	0.2	0.2	2	2	1	1.2439	1.0657
0.2	0.1	0.2	0.3	0.2	0.2	**0.4**	0.2	0.2	2	2	1	1.2070	1.4460
0.2	0.1	0.2	0.3	0.2	0.2	**0.8**	0.2	0.2	2	2	1	1.0797	1.4223
0.2	0.1	0.2	0.3	0.2	0.2	**1.2**	0.2	0.2	2	2	1	0.9599	1.3966
0.2	0.1	0.2	0.3	0.2	0.2	0.2	**0.4**	0.2	2	2	1	1.3370	1.5958
0.2	0.1	0.2	0.3	0.2	0.2	0.2	**0.8**	0.2	2	2	1	1.4551	1.8261
0.2	0.1	0.2	0.3	0.2	0.2	0.2	**1.2**	0.2	2	2	1	1.5644	2.0206
0.2	0.1	0.2	0.3	0.2	0.2	0.2	0.2	**0.4**	2	2	1	1.2743	1.4965
0.2	0.1	0.2	0.3	0.2	0.2	0.2	0.2	**0.8**	2	2	1	1.2757	1.5653
0.2	0.1	0.2	0.3	0.2	0.2	0.2	0.2	**1.2**	2	2	1	1.2770	1.6249

Table 3.2: Variable Case

λ	N	γ	M	R	Ec	α	S	ϵ	r	m	Pr	Variable Case (bvp4c)	
												$Cf_x\sqrt{Re_x}$	$\frac{Nu_x}{\sqrt{Re_x}}$
0.4	0.1	0.2	0.3	0.2	0.2	0.2	0.2	0.2	2	2	7	1.3165	3.3786
0.8	0.1	0.2	0.3	0.2	0.2	0.2	0.2	0.2	2	2	7	1.3087	3.3601
1.2	0.1	0.2	0.3	0.2	0.2	0.2	0.2	0.2	2	2	7	1.3004	3.3399
0.2	**0.4**	0.2	0.3	0.2	0.2	0.2	0.2	0.2	2	2	7	1.4906	3.5813
0.2	**0.8**	0.2	0.3	0.2	0.2	0.2	0.2	0.2	2	2	7	1.6937	3.7733
0.2	**1.2**	0.2	0.3	0.2	0.2	0.2	0.2	0.2	2	2	7	1.8761	3.9156
0.2	0.1	**0.4**	0.3	0.2	0.2	0.2	0.2	0.2	2	2	7	1.3948	3.2867
0.2	0.1	**0.8**	0.3	0.2	0.2	0.2	0.2	0.2	2	2	7	1.5312	3.1097
0.2	0.1	**1.2**	0.3	0.2	0.2	0.2	0.2	0.2	2	2	7	1.6544	2.9579
0.2	0.1	0.2	**0.4**	0.2	0.2	0.2	0.2	0.2	2	2	7	1.3592	3.3349
0.2	0.1	0.2	**0.8**	0.2	0.2	0.2	0.2	0.2	2	2	7	1.5040	3.1466
0.2	0.1	0.2	**1.2**	0.2	0.2	0.2	0.2	0.2	2	2	7	1.6348	2.9855
0.2	0.1	0.2	0.3	**0.4**	0.2	0.2	0.2	0.2	2	2	7	1.3206	3.5845
0.2	0.1	0.2	0.3	**0.8**	0.2	0.2	0.2	0.2	2	2	7	1.3213	3.9309
0.2	0.1	0.2	0.3	**1.2**	0.2	0.2	0.2	0.2	2	2	7	1.3219	4.2303
0.2	0.1	0.2	0.3	0.2	**0.4**	0.2	0.2	0.2	2	2	7	1.3119	2.6691
0.2	0.1	0.2	0.3	0.2	**0.8**	0.2	0.2	0.2	2	2	7	1.2956	1.8791
0.2	0.1	0.2	0.3	0.2	**1.2**	0.2	0.2	0.2	2	2	7	1.2796	1.4537
0.2	0.1	0.2	0.3	0.2	0.2	**0.4**	0.2	0.2	2	2	7	1.2989	3.3806
0.2	0.1	0.2	0.3	0.2	0.2	**0.8**	0.2	0.2	2	2	7	1.2565	3.3678
0.2	0.1	0.2	0.3	0.2	0.2	**1.2**	0.2	0.2	2	2	7	1.2144	3.3557
0.2	0.1	0.2	0.3	0.2	0.2	0.2	**0.4**	0.2	2	2	7	1.3797	3.6156
0.2	0.1	0.2	0.3	0.2	0.2	0.2	**0.8**	0.2	2	2	7	1.4933	4.0142
0.2	0.1	0.2	0.3	0.2	0.2	0.2	**1.2**	0.2	2	2	7	1.6000	4.3557
0.2	0.1	0.2	0.3	0.2	0.2	0.2	0.2	**0.4**	2	2	7	1.6000	4.4003
0.2	0.1	0.2	0.3	0.2	0.2	0.2	0.2	**0.8**	2	2	7	1.6001	4.4853
0.2	0.1	0.2	0.3	0.2	0.2	0.2	0.2	**1.2**	2	2	7	1.6002	4.5651

Table 3.3: Variable Case

Table 3.3 shows that, C_{fx} increases for N, γ, M, S and decreases for Ec, α. Whereas it slightly increases for R, ϵ and slightly decreases for λ. Nu_x increases for N, R, S, ϵ and decreases for Ec, α, λ, γ, M.

3.2.4 Case B: Constant Fluid Proprties

From equations (3.16) and (3.17) the system of first order is:

$$
\begin{aligned}
y_1 = f \qquad & \Rightarrow y_1^{'} = f^{'} = y_2 \ , \\
y_2 = f^{'} \qquad & \Rightarrow y_2^{'} = f^{''} = y_3 \ , \\
y_3 = f^{''} \qquad & \Rightarrow y_3^{'} = f^{'''} = \mathrm{M}y_2 + \mathrm{S}y_2 + \frac{1}{2}\mathrm{S}\eta y_3 + y_2^2 - y_1 y_3 \ , \\
y_4 = \theta \qquad & \Rightarrow y_4^{'} = \theta^{'} = y_5 \ , \\
y_5 = \theta^{'} \qquad & \Rightarrow y_5^{'} = \theta^{''} = \theta^{''} = \frac{\mathrm{Pr}}{1+\mathrm{R}} \Big(-\mathrm{Ec}y_3^2 + \frac{1}{2}y_5 \mathrm{S}\eta \\
& \qquad\qquad + \mathrm{S}y_4 \mathrm{m} + \mathrm{r}y_2 y_4 - y_1 y_5 \big) \ .
\end{aligned}
\tag{3.25}
$$

Table 3.4 demonstrates how C_{fx} and Nu_x respond to various parameters like λ, N, γ, M, R, Ec, and S. It is found that C_{fx} increases slightly for N, γ, and M. Nu_x increases slightly for N. With increasing γ and M, Nu_x reduces slightly. Nu_x increases slightly for R and decreases slightly for Ec. Nu_x and C_{fx} both slightly increase with S.

λ	N	γ	M	R	Ec	S	r	m	Pr	Constant Case ($\alpha = 0$, $\epsilon = 0$)	
										$Cf_x\sqrt{Re_x}$	$\frac{Nu_x}{\sqrt{Re_x}}$
0.4	0.1	0.2	0.3	0.2	0.2	0.2	2	2	1	1.3383	1.4231
0.8	0.1	0.2	0.3	0.2	0.2	0.2	2	2	1	1.3312	1.4200
1.2	0.1	0.2	0.3	0.2	0.2	0.2	2	2	1	1.3238	1.4167
0.2	**0.4**	0.2	0.3	0.2	0.2	0.2	2	2	1	1.5079	1.4707
0.2	**0.8**	0.2	0.3	0.2	0.2	0.2	2	2	1	1.7075	1.5160
0.2	**1.2**	0.2	0.3	0.2	0.2	0.2	2	2	1	1.8876	1.5497
0.2	0.1	**0.4**	0.3	0.2	0.2	0.2	2	2	1	1.4208	1.3991
0.2	0.1	**0.8**	0.3	0.2	0.2	0.2	2	2	1	1.5667	1.3537
0.2	0.1	**1.2**	0.3	0.2	0.2	0.2	2	2	1	1.6997	1.3140
0.2	0.1	0.2	**0.4**	0.2	0.2	0.2	2	2	1	1.3818	1.4116
0.2	0.1	0.2	**0.8**	0.2	0.2	0.2	2	2	1	1.5316	1.3644
0.2	0.1	0.2	**1.2**	0.2	0.2	0.2	2	2	1	1.6675	1.3234
0.2	0.1	0.2	0.3	**0.4**	0.2	0.2	2	2	1	1.3417	1.5129
0.2	0.1	0.2	0.3	**0.8**	0.2	0.2	2	2	1	1.3417	1.6656
0.2	0.1	0.2	0.3	**1.2**	0.2	0.2	2	2	1	1.3417	1.7957
0.2	0.1	0.2	0.3	0.2	**0.4**	0.2	2	2	1	1.3417	1.3214
0.2	0.1	0.2	0.3	0.2	**0.8**	0.2	2	2	1	1.3417	1.1542
0.2	0.1	0.2	0.3	0.2	**1.2**	0.2	2	2	1	1.3416	1.0246
0.2	0.1	0.2	0.3	0.2	0.2	**0.4**	2	2	1	1.4003	1.5581
0.2	0.1	0.2	0.3	0.2	0.2	**0.8**	2	2	1	1.5127	1.7833
0.2	0.1	0.2	0.3	0.2	0.2	**1.2**	2	2	1	1.6187	1.9751

Table 3.4: Constant Case ($\alpha = 0$, $\epsilon = 0$)

λ	N	γ	M	R	Ec	S	r	m	Pr	Constant Case ($\alpha = 0$, $\epsilon = 0$)	
										$Cf_x\sqrt{Re_x}$	$\frac{Nu_x}{\sqrt{Re_x}}$
0.4	0.1	0.2	0.3	0.2	0.2	0.2	2	2	7	1.3382	3.3419
0.8	0.1	0.2	0.3	0.2	0.2	0.2	2	2	7	1.3312	3.3255
1.2	0.1	0.2	0.3	0.2	0.2	0.2	2	2	7	1.3238	3.3079
0.2	**0.4**	0.2	0.3	0.2	0.2	0.2	2	2	7	1.5079	3.5358
0.2	**0.8**	0.2	0.3	0.2	0.2	0.2	2	2	7	1.7075	3.7223
0.2	**1.2**	0.2	0.3	0.2	0.2	0.2	2	2	7	1.8876	3.8617
0.2	0.1	**0.4**	0.3	0.2	0.2	0.2	2	2	7	1.4208	3.2480
0.2	0.1	**0.8**	0.3	0.2	0.2	0.2	2	2	7	1.5667	3.0684
0.2	0.1	**1.2**	0.3	0.2	0.2	0.2	2	2	7	1.6997	2.9137
0.2	0.1	0.2	**0.4**	0.2	0.2	0.2	2	2	7	1.3818	3.2978
0.2	0.1	0.2	**0.8**	0.2	0.2	0.2	2	2	7	1.5316	3.1107
0.2	0.1	0.2	**1.2**	0.2	0.2	0.2	2	2	7	1.6675	2.9504
0.2	0.1	0.2	0.3	**0.4**	0.2	0.2	2	2	7	1.3416	3.5528
0.2	0.1	0.2	0.3	**0.8**	0.2	0.2	2	2	7	1.3416	3.9068
0.2	0.1	0.2	0.3	**1.2**	0.2	0.2	2	2	7	1.3416	4.2107
0.2	0.1	0.2	0.3	0.2	**0.4**	0.2	2	2	7	1.3416	2.6342
0.2	0.1	0.2	0.3	0.2	**0.8**	0.2	2	2	7	1.3416	1.18457
0.2	0.1	0.2	0.3	0.2	**1.2**	0.2	2	2	7	1.3416	1.4205
0.2	0.1	0.2	0.3	0.2	0.2	**0.4**	2	2	7	1.4003	3.5772
0.2	0.1	0.2	0.3	0.2	0.2	**0.8**	2	2	7	1.5127	3.9750
0.2	0.1	0.2	0.3	0.2	0.2	**1.2**	2	2	7	1.6187	4.3163

Table 3.5: Constant Case ($\alpha = 0$, $\epsilon = 0$)

Table 3.5 shows that, C_{fx} increases for N, γ, M, S. Nu_x decreses for λ, γ, M, Ec and increases for N, R, S.

3.3 Graphical Analysis

We will analyze the variable case graphically in this section. We will look at the behaviour of dimensionless velocity $f^{'}(\eta)$ and dimensionless temperature $\theta(\eta)$ along different parameters such as λ, N, γ, R, Ec, α, S, ϵ.

Figure 3.2 shows that $\theta(\eta)$ first increases and then decreases with the rising vales of thermal radiation parameter R.

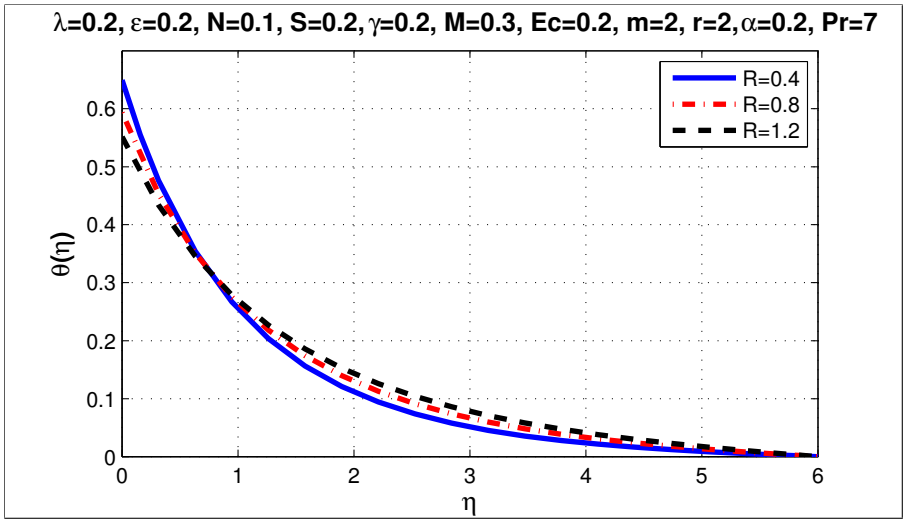

Figure 3.2: Analysis of temperature for R and its distribution.

From the **Figure 3.3(a)** it can be seen that $f^{'}(\eta)$ decreases along the increasing values of M and thickness of momentum boundary layer reduces with it as well. While $\theta(\eta)$ is increased for the increased values of M and thermal boundary layer thickens with it. **Figure 3.3(b)**.

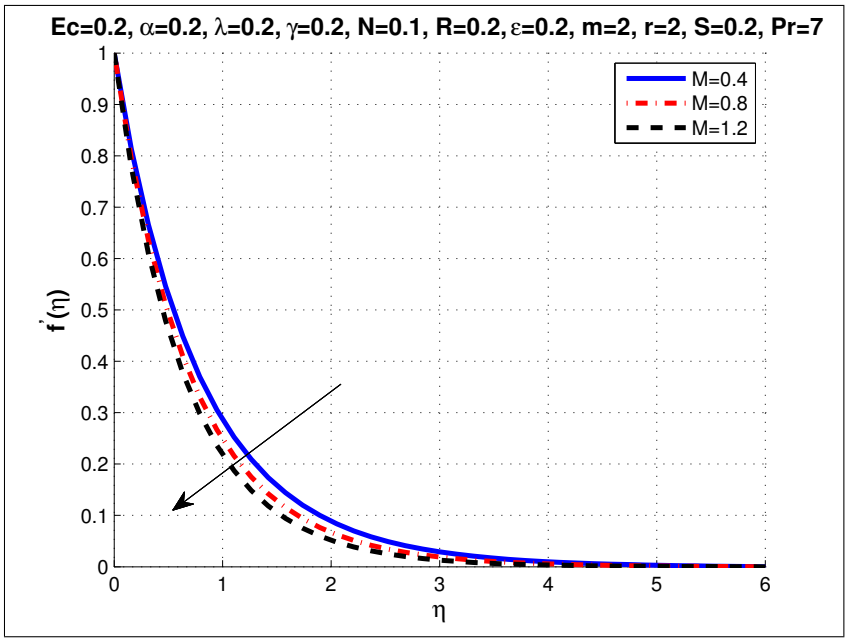

(a)

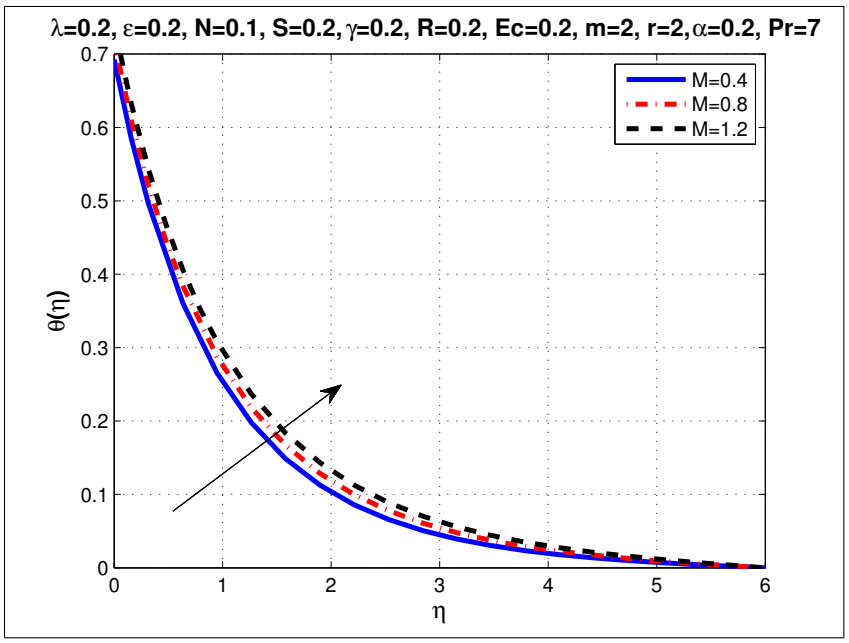

(b)

Figure 3.3: (a) Analysis of velocity for M and its distribution. (b) Analysis of temperature for M and its distribution.

Figure 3.4 demonstrates that when Eckert number Ec grows, $\theta(\eta)$ increases and thermal boundary layer thickness increases as well.

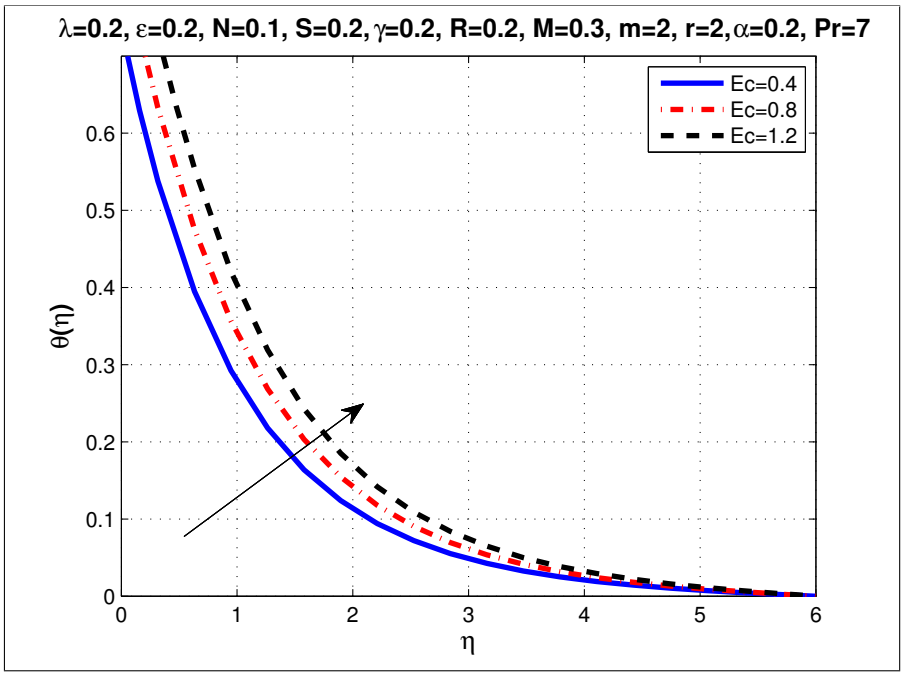

Figure 3.4: Analysis of temperature for Ec and its distribution.

When the value of the thermal conductivity parameter ϵ increases, the temperature distribution increases along the parameter ϵ, as seen in **Figure 3.5**.

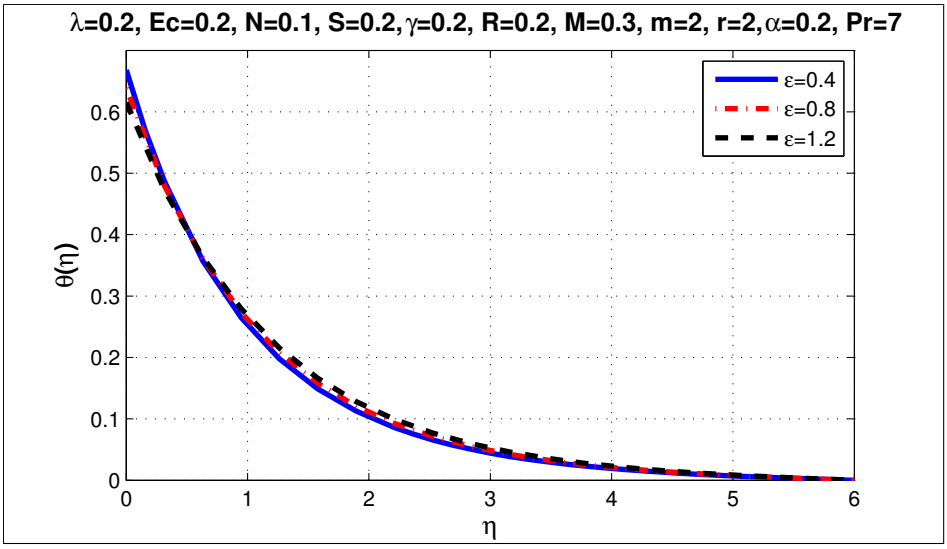

Figure 3.5: Analysis of temperature for ϵ and its distribution.

In **Figure 3.6(a) and 3.6(b)**, we have plotted the dimensionless velocity and dimensionless temperature with increasing viscosity parameter α. As illustrated in **Figure 3.6(a)**, $f'(\eta)$ decreases with a slight decrease in momentum boundary layer thickness, as α increases, while $\theta(\eta)$ increases as α increases **Figure 3.6(b)**.

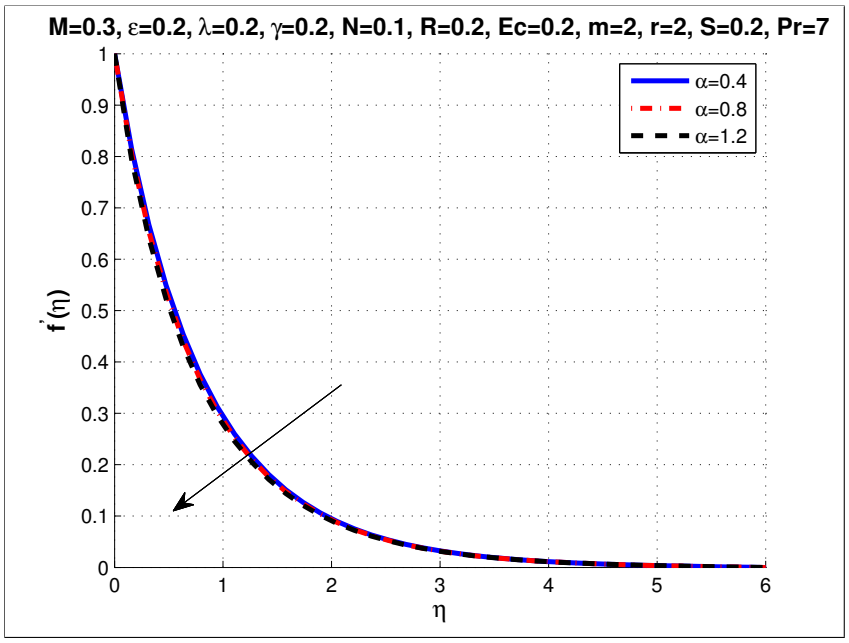

(a)

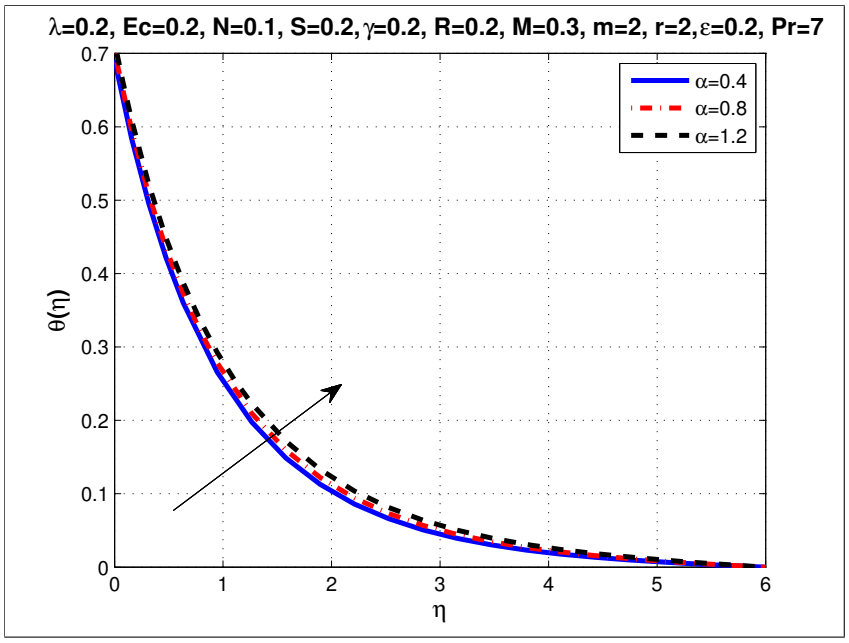

(b)

Figure 3.6: (a) Analysis of velocity for α and its distribution. (b) Analysis of temperature for α and its distribution.

Figure 3.7(a) shows the effect of increasing the value of unsteadiness parameter S on the velocity profiles, as S increases, $f^{'}(\eta)$ decreases. Similarly, **Figure 3.7(b)** shows that an increase in the value of S will reduce the $\theta(\eta)$ and thermal boundary layer thickness reduces .

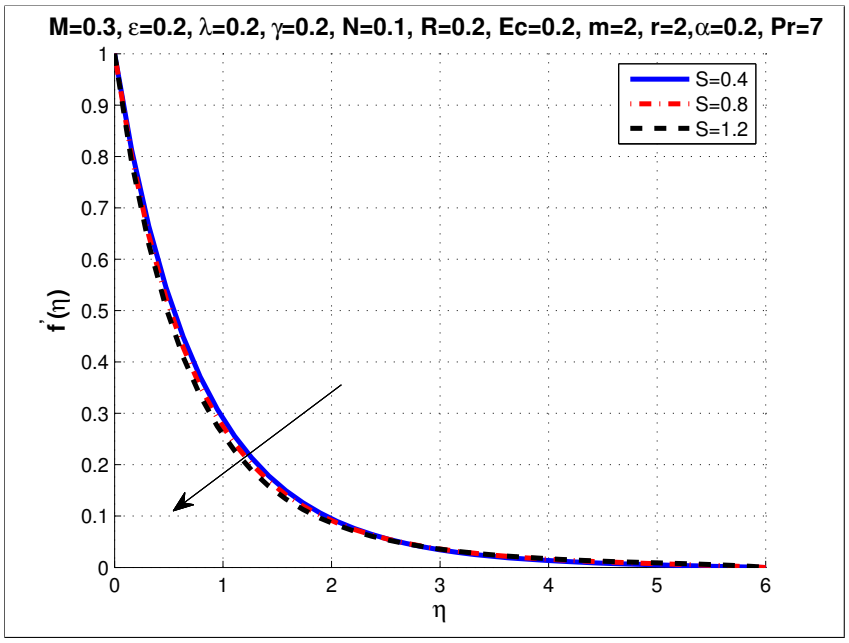

(a)

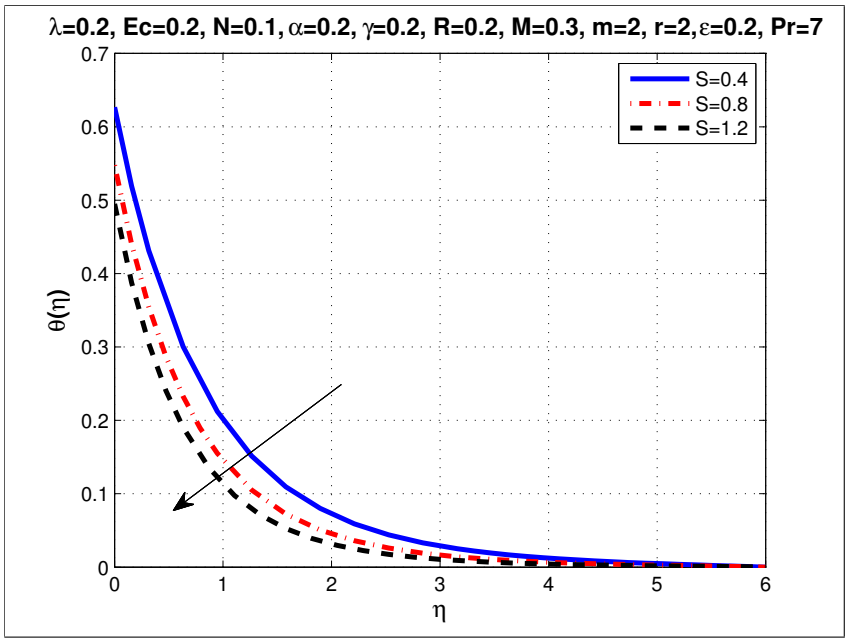

(b)

Figure 3.7: (a) Analysis of velocity for S and its distribution. (b) Analysis of temperature for S and its distribution.

The dimensionless velocity diminishes as the value of darcy number γ increases, as shown in **Figure 3.8** and momentum boundary layer thickness reduces.

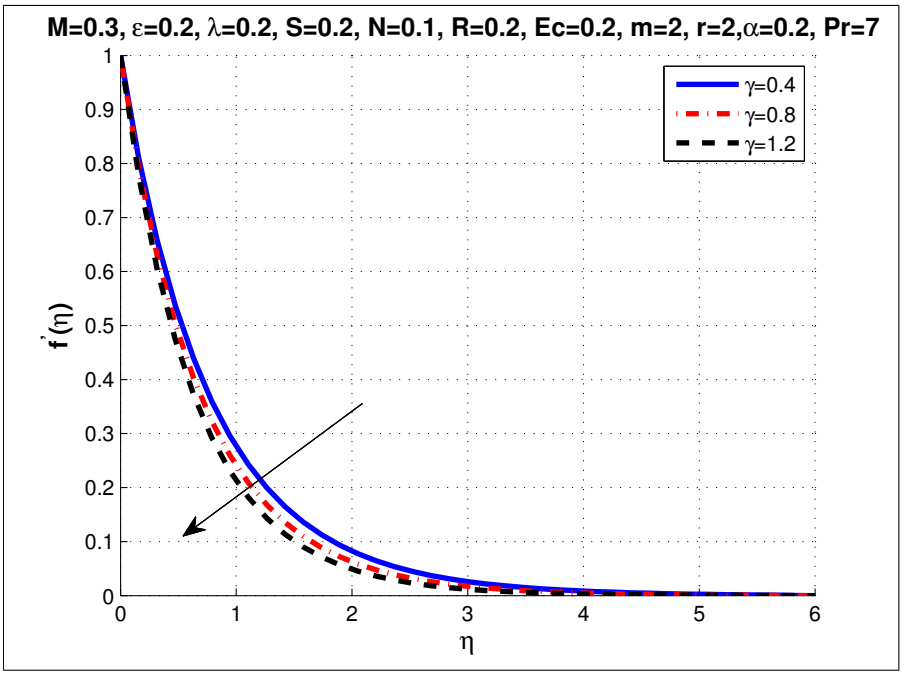

Figure 3.8: Analysis of velocity for γ and its distribution.

The influence of the fluid parameter N on the dimensionless velocity curves is shown in **Figure 3.9**.

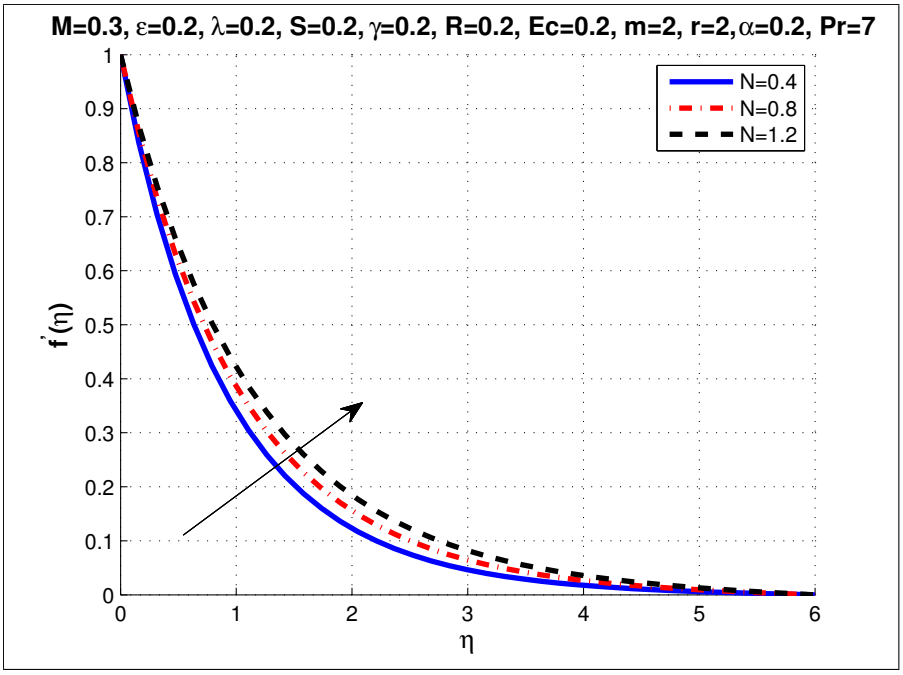

Figure 3.9: Analysis of velocity for N and its distribution.

In **Figure 3.10**, we prefer to explore the effects of free stream parameter λ on the velocity profiles.

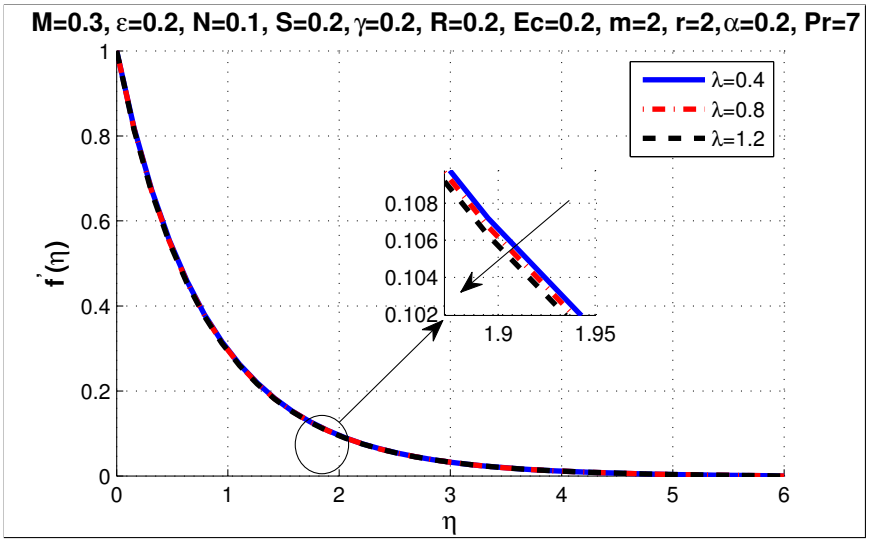

Figure 3.10: Analysis of velocity for λ and its distribution.

Chapter 4

Conclusions

A brief historical background is given in chapter one, along with some basic definitions and fundamental laws, such as, such as Newtonian and non-Newtonian fluids, compressible and incompressible flow, steady and unsteady flow, MHD flow, and mass, momentum, and energy conservation. Non dimensional parameters such as the Reynolds number, Prandtl number, Nusselt number, and Eckert number have also been defined. At last, a brief description of *bvp4c* has been given.

In chapter two, we look at an unstable stretching sheet with an extended heat flow problem, which is causing the MHD fluid boundary layer laminar flow and heat transfer. Using similarity variables, the ODEs are converted into PDEs. The ODEs are then solved with *bvp4c*, and the results are plotted and presented in tabular form. The behaviour of dimensionless temperature and velocity, skin friction coefficient and local Nusselt number, is investigated in relation to the various parameters.

In chapter Three, the flow and heat transfer of a non-Newtonian fluid across an unstable stretching sheet is investigated. The movement of which is caused by a stretching sheet. Numerical solutions for momentum and heat transfer are obtained by employing *bvp4c* in matlab. In the presence of the magnetic parameter M, tables and graphs were utilised to examine dimensionless velocity, dimensionless temperature, local Nusselt number and skin friction coefficient, thermal radiation parameter R, Eckert number

Ec, and viscosity parameter α, S is the stability parameter, and free stream parameter λ, Darcy number γ, fluid parameter N and variable thermal conductivity ϵ.

1. The comparison of skin friction coefficient in our study with Prasad et al. [11] and Megahed et al. [12] is listed in Table 3.

2. From section 4, we observe that the momentum boundary layer thickness reduces slightly for M, α, S, γ, and increases for N.

3. We also notice that the thermal boundary layer thickness increases with Eckert number Ec, and it also increases slightly with M and α. In the case of S, however, it decreases.

4. It can be observed that the skin friction coefficient C_{fx} is more in constant case as compared to in variable case.

Bibliography

[1] Shang, J. S. *Three Decades Of Accomplishments In Computational Fluid Dynamics*. Progress in Aerospace Sciences, **40**, 173, (2004).

[2] Richardson LF. *The Approximate Arithmetical Solution By Finite Differences Of Physical Problems Involving Differential Equations, With An Application To The Stresses In A Masonry Dam*. Phil Trans R Soc London, Series A, **210**, 307, (1910).

[3] von Neumann J, Richtmeyer RD. *A Method For The Numerical Calculation On The Hydrodynamic Shocks*. J Appl Phys, **21**, 232, (1950).

[4] Godunov SK. *Finite-Difference Method For Numerical Computational Of Discontinuous Solution Of The Equations of fluid dynamics*. Mat Sb, **47**, 271, (1959).

[5] Roache PJ. *Computational Fluid Dynamics*. Albuquerque, NM: Hermosa Publishers, (1976).

[6] Tannehill JC, Anderson DA, Pletcher RH. *Computational Fluid Mechanics And Heat Transfer*. Philadelphia, PA: Taylor Francis, (1997).

[7] Raju, K. S. *Fluid Mechanics, Heat Transfer, And Mass Transfer: Chemical Engineering Practice*. John Wiley , Sons, (2011).

[8] Young, D. F., Munson, B. R., Okiishi, T. H., , Huebsch, W. W. *A Brief Introduction To Fluid Mechanics*. John Wiley , Sons, (2010).

[9] Yunus A.. ÃĞengel, , John M.. Cimbala. *Fluid Mechanics: Fundamentals And Applications.* McGraw-Hill Higher Education, (2010).

[10] Landau, L. D., , Lifshitz, E. M. *Magnetohydrodynamics.* Electrodynamics Of Continuous Media, (1984).

[11] Fagbenle, R. O., Olaleye Michael Amoo, Ayodeji Falana, and Sufianu Aliu, eds. Applications Of Heat, Mass And Fluid Boundary Layers. Woodhead Publishing Limited, 2020.

[12] Petrila, T., Trif, D.. *Basics Of Fluid Mechanics And Introduction To Computational Fluid Dynamics.* Springer Science , Business Media, (2004).

[13] Kundu, P. K., Cohen, I. M., , Dowling, D. R. *Fluid Mechanics, 5th Version.* Academic, Berlin, (2012).

[14] Gray, D. D., , Giorgini, A. *The Validity Of The Boussinesq Approximation For Liquids And Gases.* International Journal Of Heat And Mass Transfer, **19**, 545, (1976).

[15] Mahmoud, M. A. A., Megahed, A. M. *MHD Flow And Heat Transfer In A Non-Newtonian Liquid Film Over An Unsteady Stretching Sheet With Variable Fluid Properties.* Canadian Journal Of Physics, **87**, 1065, (2009)

[16] Liu, I.-C., Megahed, A. M., , Wang, H.-H. *Heat Transfer In A Liquid Film Due To An Unsteady Stretching Surface With Variable Heat Flux.* Journal Of Applied Mechanics, **80**, 041003, (2013).

[17] Prasad, K., K. Vajravelu, P. S. Datti and B. Raju. âĂIJMHD Flow And Heat Transfer In A Power-law Liquid Film At aA Porous Surface In The Presence Of Thermal Radiation.âĂİ Journal Of Applied Fluid Mechanics 6 (2013): 385-395.

[18] Dandapat, B. S., Santra, B., , Vajravelu, K. *The Effects Of Variable Fluid Properties And Thermocapillarity On The Flow Of A Thin Film On An Unsteady Stretching Sheet*. International Journal Of Heat And Mass Transfer, **50**, 991, (2007).

[19] Prasad, K. V., Dulal Pal, and P. S. Datti. "MHD Power-Law Fluid Flow And Heat Transfer Over A Non-Isothermal Stretching Sheet." Communications In Nonlinear Science And Numerical Simulation 14, no. 5 (2009): 2178-2189.

[20] Megahed, Ahmed M., M. Gnaneswara Reddy, and W. Abbas. "Modeling Of MHD Fluid Flow Over An Unsteady Stretching Sheet With Thermal Radiation, Variable Fluid Properties And Heat Flux." Mathematics And Computers In Simulation 185 (2021): 583-593.

[21] Schlichting, Hermann, and Klaus Gersten. Boundary-layer theory. Springer, 2016.